Modeling Uprighting of the Orion Crew Module using a Finite Element Method with Wave Coupling and Structural Deformability

John Puryear[1] and Shreyas Joglekar[2]
Applied Physical Sciences Corporation, Groton, CT, 06340, USA

Tannen VanZwieten[3]
NASA Engineering and Safety Center, Kennedy Space Center, FL, 32899, USA

Troy Lyons[4]
NASA Glenn Research Center, Cleveland, OH, 44135, USA

Abstract

The Crew Module Uprighting System (CMUS) for the Orion Crew Module (CM) consists of five bags and tethers that deploy and inflate after splashdown to upright the CM if it overturns during or after landing. Wave conditions can be severe enough to damage the CMUS bags and tethers, which could impact the system's ability to upright the CM. Thus, the CMUS design capability must exceed the maximum load that will be observed in environmental conditions where the CM is expected to land. This paper describes a full fluid-structure interaction computational model being used to evaluate CMUS loads in a variety of wave environments. This finite element model uses explicit time integration to directly simulate uprighting, a computational approach usually reserved for short duration, highly transient phenomena. The approach is determined to be a feasible solution for simulating CMUS uprighting and estimating the loads the CMUS tethers experience in a variety of wave conditions. The results will be used to provide synthetic data that supplement the available experimental data being used to verify and validate the baseline model in support of NASA's Artemis program.

I. Nomenclature

C	=	speed of sound
δ_{ij}	=	Kronecker delta
D_{ij}	=	i^{th}, j^{th} deviatoric stress
η	=	viscosity
μ	=	volumetric strain
ρ	=	density
ρ_0	=	initial density
t	=	time
T_{ij}	=	Cauchy stress tensor

[1] Senior Engineer – Group Manager, Structural Mechanics
[2] Senior Engineer, Structural Mechanics
[3] Associate Principal Engineer, AIAA Member
[4] Aerospace Engineer, Structural Dynamics Branch, AIAA Member

II. Introduction

The Orion Crew Module (CM) is equipped with a Crew Module Uprighting System (CMUS) intended to rotate the CM to the upright (Stable 1) position if it overturns during or after landing. The CMUS consists of five deployable, 55-inch diameter uprighting bags, as shown in Fig. 1, that are each attached to the CM using four main and four base tethers. The CMUS must upright the CM in wave conditions that could occur during nominal and abort landing scenarios without exceeding allowable peak loads on the bags and tethers. This paper describes the modeling approach and simulations that were run in the commercial finite element software LS-DYNA® to predict tether loads. The work was conducted to establish the feasibility of this approach and estimate loads to supplement previous computational and experimental data obtained for CMUS.

Fluids and solids in the CMUS finite element model were handled in different ways numerically within the simulations. Solids (including the CMUS softgoods, i.e. tethers and bags) were modeled as Lagrangian [1-3] parts, where each mesh deforms with the structures. This is the approach used in conventional structural finite element analysis. The ocean water and helium in the bags, in contrast, were modeled with the Arbitrary Lagrangian Eulerian (ALE) [1-3] approach, where the water and helium move through the numerical mesh instead of with it. The use of ALE avoids the numerical ill-conditioning that would occur if the mesh becomes greatly distorted, which would occur from applying a Lagrangian approach to fluid dynamics.

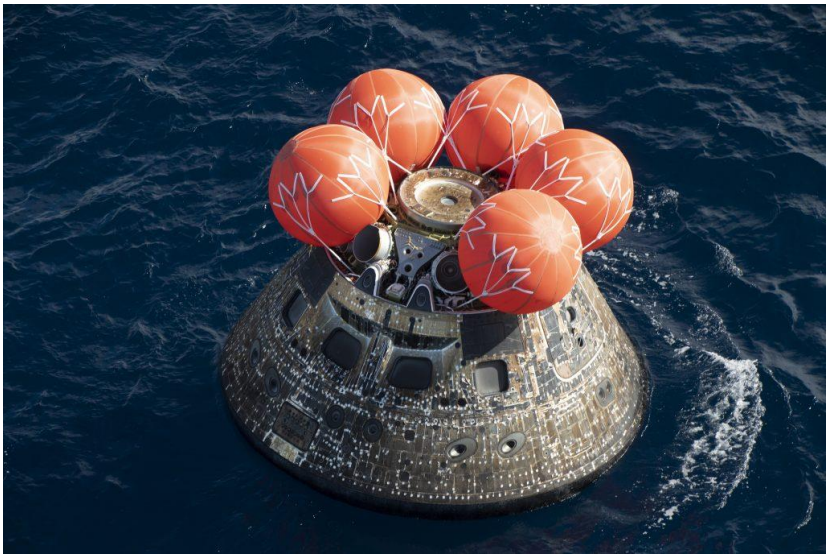


Fig. 1 Orion CM with inflated CMUS bags in the Stable 1 (upright) orientation, at the end of the Artemis I mission [4]

This paper discusses the ALE methodology that was leveraged in Section III, followed by a description of the CM model (inclusive of the CMUS) in Section IV. The design waves and how they were generated in the ALE domain are discussed in Section V. The relevant Lagrangian structure, geometry, material models and element formulations used for the CM and CMUS are described in Section VI. In Section VII, the uprighting performance of the CMUS for a set of design waves is compared to test cases using wave inputs that match uprighting tests conducted in the Atlantic Ocean. Finally, results in more challenging design wave scenarios are provided in Section VIII.

III. ALE Methodology

The ALE method is an adaption of the FEM for accommodating large deformations that would cause excessive mesh distortion in a purely Lagrangian model. For each timestep, the parts of an ALE model deform according to a Lagrangian element formulation. However, ALE includes an advection step every specified number of timesteps to remap the points constituting the domain to their initial position. Material points continue advancing without remapping and can consequently displace arbitrarily. ALE combines the desirable characteristics of Eulerian solvers (large deformations) and Lagrangian solvers (well-defined interfaces between parts). The method is useful for modeling fluids and their interactions with structures.

Despite its capability to model fluid-structure interaction (FSI), explicit finite element method (FEM) analysis (especially with ALE) is typically reserved for simulations of events that are tenths of seconds. This practice is common because the maximum timestep is limited by the Courant stability condition, which is necessary for solving the governing equations. The condition relates wave speed in the material and element length to imply a limiting timestep. Increasingly dense meshes not only create larger finite element models, but they also have smaller elements that in turn drive down the maximum allowed timestep. Compared with other methods, such as spectral approaches, ALE converges slowly as a function of element size [5]. It consequently can have a restrictive stability condition, i.e. small timestep, that can make clock times to complete calculations impractically long.

Alternative methods to ALE for non-transient hydrodynamic problems lack the capability to model deformability, especially if the deformations are nonlinear. Modeling deformability is required to characterize the CMUS given its inclusion of flexible structures. In addition, the fact that ALE is commonly used for mechanical shock and projectile impact problems suggests it as a potential method for modeling the dynamics of wave impact. The potential for ALE to model the critical parts of the CMUS is illustrated in Fig. 2. The figure is stills of a CMUS bag being released in a container of water, rising due to buoyant force and impacting the top of the container. Therefore, because ALE in principle has the features required to model uprighting of the CM due to the CMUS (i.e., fluid interaction with deformable, fabric structures) it was selected for further investigation.

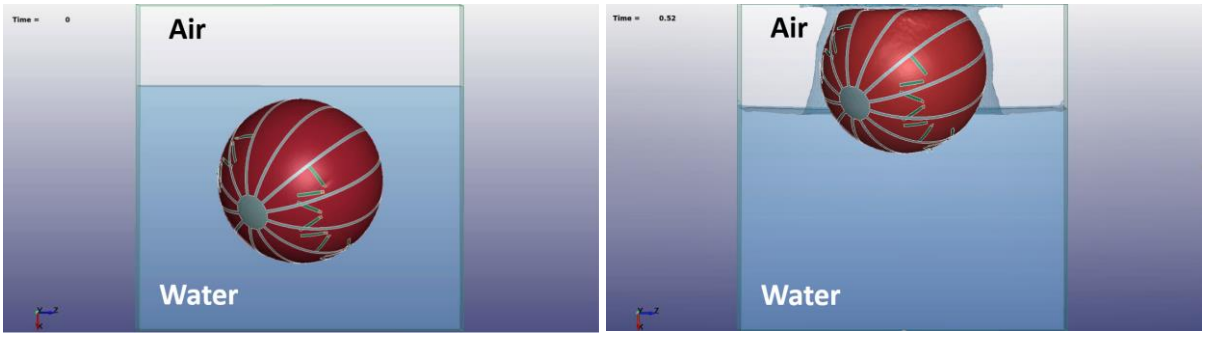


Fig. 2. Example of deformability of softgoods in ALE interacting with FEM parts

IV. LS-DYNA Model Details

Details of the LS-DYNA calculation include modeling the CMUS bags with fully-integrated Belytschko-Tsay membrane shell elements [1-3]. Fully-integrated elements (as opposed to constant stress elements) do not include hourglass modes [1,3], which are deformation without associated internal energy, a non-physical condition. They do, however, have higher computational cost and exhibit decreased robustness for large deformations. Deformations in the CMUS calculations were not large enough for the latter limitation to cause instability, and fully-integrated elements were accordingly used. Furthermore, membrane elements were chosen because they only have one through-thickness integration point. This condition reduces computational cost and provides an adequate approximation for thin fabrics. The fabric of the CMUS bags is thin and unable to support bending (which has a variable stress state through the shell thickness), such that a single integration point through the thickness is sufficient.

Within LS-DYNA, the newer structured ALE solver was used. It is recommended for cases where the ALE mesh can be a regular grid. The structured ALE solver has some internal optimizations that take advantage of a regular, grid mesh for increased speed and FSI. When using ALE, the domain is filled with a particular species, in this case the air, and the other species (water and helium in the bags) are defined by subdomains. The CM and each CMUS bag act as containers to define the subdomains of the water and helium. The CMUS bags were approximated as being fully inflated through the entirety of the simulation. This approach makes uprighting occur earlier in the simulation than if the bags were inflated during uprighting, as occurs in actual deployment of the CM. The effects of gravity, including the buoyant force and hydrostatic pressure, were initialized to reduce artificial oscillation from the sudden application of gravity at the beginning of the simulation.

The material model used for the water included an equation of state and viscosity. Viscosity is important in hydrodynamic applications like uprighting. For the equation of state, pressure is a function of the non-dimensional volumetric strain, μ,

$$\mu = {\rho(t)}/{\rho_0} - 1 \qquad (1)$$

where ρ, ρ_0, t, are the density, initial density, and time, respectively. Eq. 1 can also be written as the ratio of current to initial volume of an element. A simplified Grüniesen equation [3,6] of state was used, where the relationship between pressure, p and μ is defined in Eq. 2,

$$p(\mu) = \rho_0 C^2 \mu \qquad (2)$$

where C = speed of sound in water = $5.906(10^4)$ in/s.

The Cauchy stress tensor, T_{ij}, can be put in terms of the pressure and viscosity, as in Eq. 3. For the uprighting simulations, the viscosity was $\eta = 1.29(10^{-7})$ psi-s [7]. Eq. 3 is written using indicial notation. The term $(D_{ij} - (1/3)D_{kk})$ is deviatoric (has zero for its trace), where D_{ij} is the symmetric part of the velocity gradient.

$$T_{ij} = -p(\mu)\delta_{ij} + 2\eta(D_{ij} - (1/3)D_{kk}) \qquad (3)$$

V. Design Wave Definition and Wave Generation in LS-DYNA using ALE

The Orion CMUS must perform in sea conditions at candidate sites for landing or abort splashdown. A set of wave spectra from buoy data was identified by the NASA Natural Environments group within the Design Specification for Natural Environments (DSNE) to define a range of wave conditions in the frequency domain that include near-bounding environments. Eight spectra were selected as representative of set of wave spectra: DSNE 2, 4, 6, 7, 8, 9, and 11. The cases also included measurements from an actual uprighting test, termed the Atlantic case. For each DSNE case, 10-minute wave histories were calculated with a high-order spectral (HOS) solver [8]. In this way, time-domain waves were generated by using a set of wave heights and frequencies corresponding to the wave spectra, and then assigned random phases and summed to produce a wave train. A process for determining near-bounding design waves for a given wave spectra was defined in [9], and this experience was leveraged for the development of design waves from the aforementioned spectra.

To control clock times when running LS-DYNA, the 60-second segment of the 10-minute elevation history containing maximum wave elevation was prescribed to the boundary of the free surface in LS-DYNA. In this way, LS-DYNA was simulated for no more than 60 seconds. Example wave trains are provided in Fig. 3 for the entire 10 minutes and for the 60-seconds selected as a wave input. DSNE 11 was an exception in that only a 60-second wave history could be simulated in the HOS solver, rather than the full 10 minutes, and this entire 60-second history was applied in LS-DYNA.

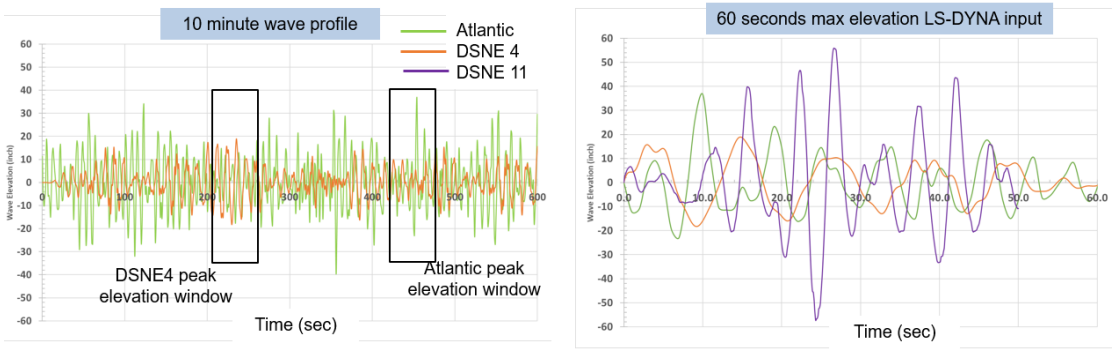


Fig. 3. Sample histories of wave elevation versus time: 10-minute wave profile and down-selected 60-seconds intended to include the maximum wave height

Fig. 4 is an illustration of the wave history prescribed at the boundary of the water domain in LS-DYNA. To confirm that ALE is adequate for generating the prescribed waves, the wave histories from the HOS were replicated in LS-DYNA for 2D and 3D cases. The wave elevations at probes in LS-DYNA were then compared to the probe values output from the HOS method. The CM was not included in these simulations. Results of this comparison, which show good agreement in amplitude and period, are provided in Fig. 5.

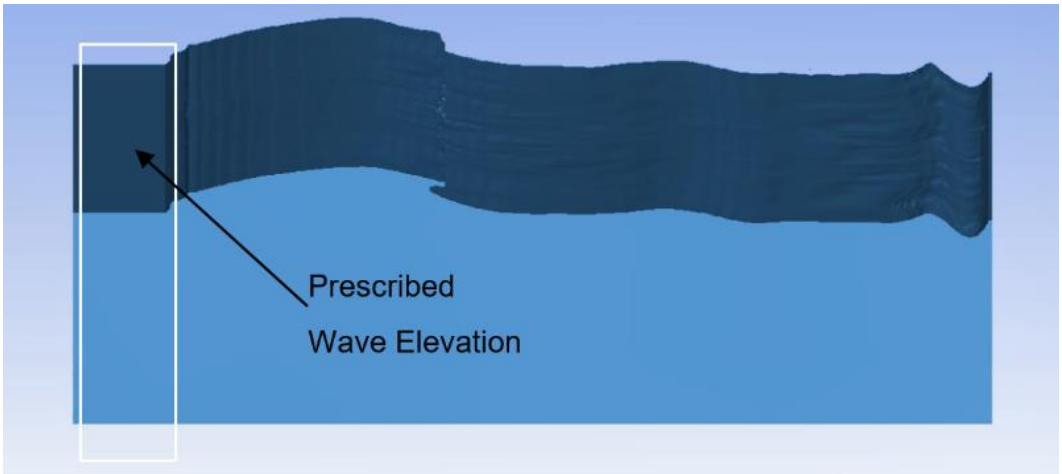


Fig. 4. Prescribed vertical wave displacement at the boundary

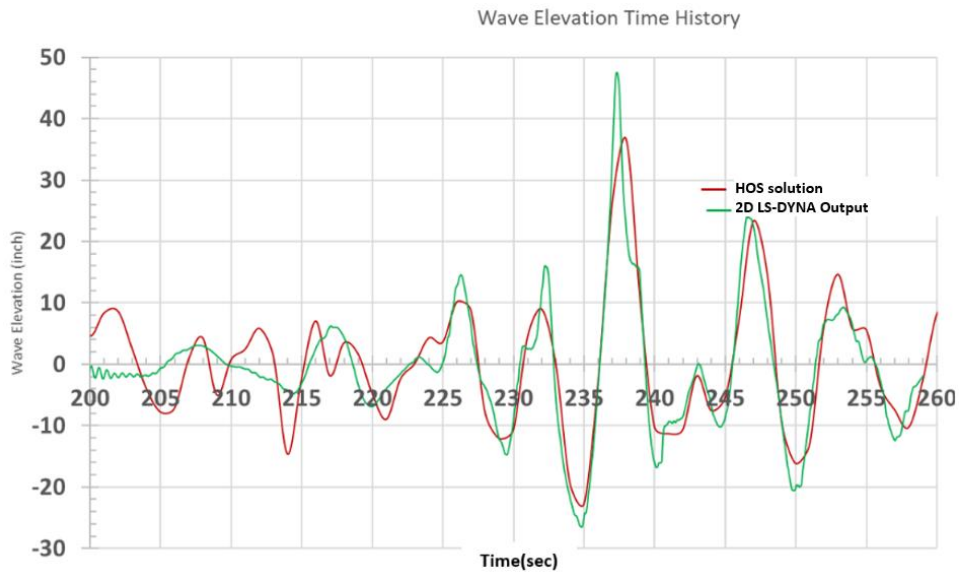


Fig. 5. Comparison of HOS solution and LS-DYNA output

VI. Structural Model for CMUS

Once the adequacy of the ALE method for representing the waves was established, the Lagrangian model of the CM and CMUS, illustrated in Fig. 6 with bag identifiers, was added to the ALE domain modeling the wave environment shown in Fig. 4. The CM was modeled with shell elements and as a rigid material, since the deformation of the "softgoods" and water dominate in comparison to the deformation to the metallic CM. The CM's mass properties were prescribed to match values of the CM's full-scale test article that was used for seakeeping tests.

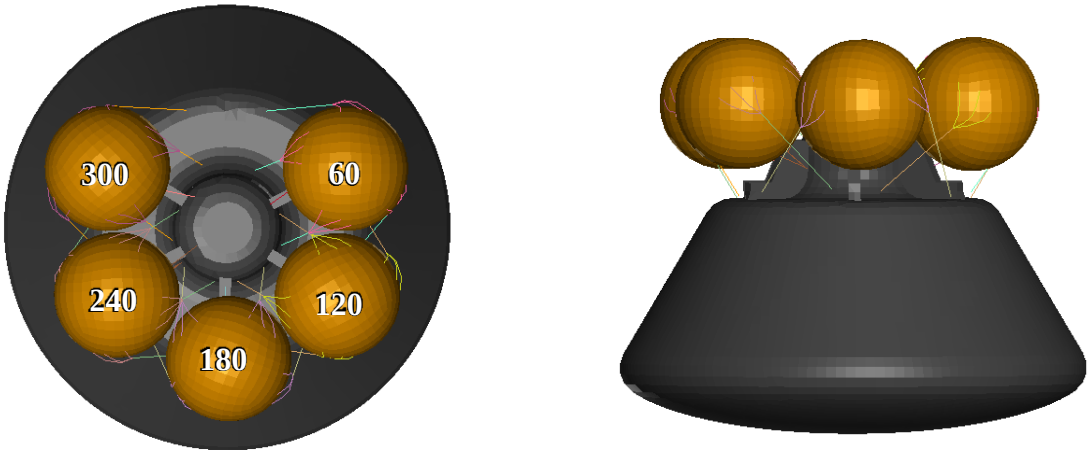


Fig. 6. Finite element model of the CM and the five CMUS bags

The CMUS bags are made of an inner liner to contain the helium gas and a fabric exterior to provide structural strength and stiffness. The liner was neglected in the LS-DYNA model, and the fabric exterior was modeled with shell elements having uniform thickness of 0.01 inches. The material model used for the bag fabric was *MAT_034M/*MAT_FABRIC_MAP. *MAT_034M is an updated version of *MAT_FABRIC, which allows for finite linear stiffness in tension, and zero stiffness in compression. This captures the effect of local buckling of the fabric fibers that macroscopically prevents the bag from resisting compression.

The tethers were modeled with one-dimensional beam elements. This approach is adequate because the stresses aside from tension in the tether's length direction, along with the tether's cross sectional area in terms of contact mechanics, are negligible. The approach has the additional advantage of avoiding mesh tangling that can result from excessive deformation of shell or solid elements in fabric materials. The material model for the tethers within LS-DYNA was *MAT_071/*MAT_CABLE_DISCRETE_BEAM. This material model allowed the structural behavior of stiffness in tension, with negligible stiffness of tether buckling under compression, to be fully modeled macroscopically. Beam element sizes varied from four to eight inches. Beam elements were ommited from the fluid structure interaction for simplicity.

Within the uprighting simulations, the CM was initially rotated 70º from the water plane, as shown in Fig. 7. Waves were created during a four-second initialization phase. The water elevation was prescribed as a function of time, and the CM was held fixed during this initialization phase. The system was simulated in LS-DYNA by advancing the calculation in time to get the response of the CM and the fluids. The wave generation varied depending upon which desired sea state was being simulated. No damping was added to the model; instead, post-processing was conducted to isolate the desired effects. Further discussion of the post-processing of the results is provided in the next section.

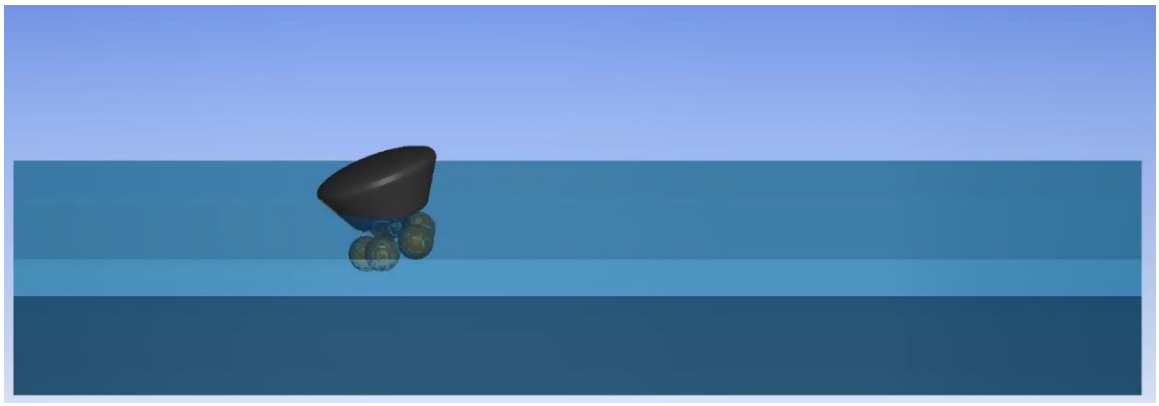


Fig. 7. The CM (including the CMUS) at its initial position in the ALE domain

VII. Comparison of Calculations to Test Measurements

As noted above, the focus of this study has been to quantify the effect of wave arrival on the loads in the tethers. The peak loads imposed on the tethers cannot exceed the capability, which is a key design driver for the bag and tethers constituting the CMUS. Prior to evaluating this requirement via LS-DYNA predicted loads, uprighting calculations were performed for comparison against experimental loads from uprighting tests conducted in NASA's Neutral Buoyancy Laboratory at Johnson Space Center and in the Atlantic Ocean [10, 11]. A still form an at-sea modeling case is shown in Fig. 8.

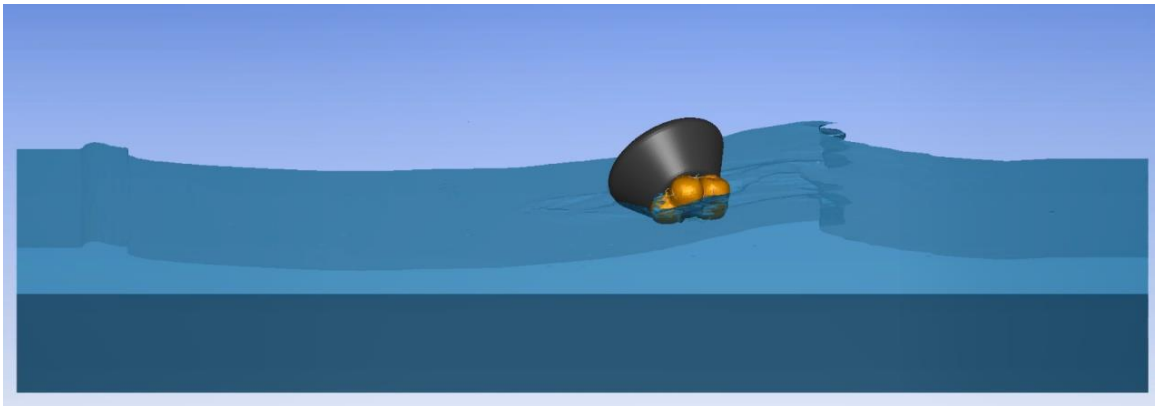


Fig. 8. CM uprighting in at-sea conditions

The tether load history was sampled from LS-DYNA at 100 Hz, the frequency used in the test measurements. Calculated loads had extensive noise due to the absence of damping. No measurement or estimate of damping was available for inclusion in the LS-DYNA calculation. To resolve the noise in the output, it was filtered as part of postprocessing.

Interpreting the results involved distinguishing between two types of loads, denoted as "rigid body" and "dynamic" loads. The rigid body loads are caused by bag inflation, buoyancy and CM uprighting. These are the loads that would generally be present during an uprighting in calm water. They are lower frequency compared to the dynamic loads and are extracted from the raw data using a low-pass filter (LPF). The same cutoff frequency was selected to postprocess the measurements as was used to determine rigid body loads.

The dynamic loads consist mostly of loads applied to the tethers by wave action. These are obtained from the raw data using a bandpass Butterworth filter (4^{th} order, backward and forward). The lower frequency defining the band was equal to the maximum frequency included in the rigid body LPF. The upper frequency of the band was chosen to be higher than the frequency range wave energy observed in the at-sea loads data. This value was also selected to be an upper bound on the anticipated natural frequencies of the CM during uprighting. In that way, any frequencies above these physically possible values were judged to be numerical artifacts. The raw data and relevant filtered histories from this approach are illustrated in Fig. 9. The blue line in the figure is an estimate of the total force seen by the example tether.

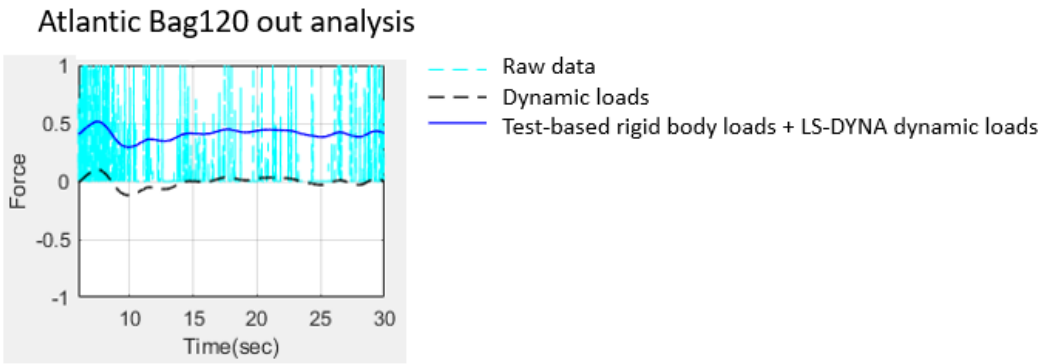


Fig. 9. Sample load time history data from the CMUS finite element model in one of the CMUS tethers

This approach to the postprocessing was followed for the tether load histories obtained for the NBL tests. The flat-water histories only included the rigid body loads. The calculated histories are shown in Fig. 10 as dashed lines, and the measured histories as solid, both normalized.

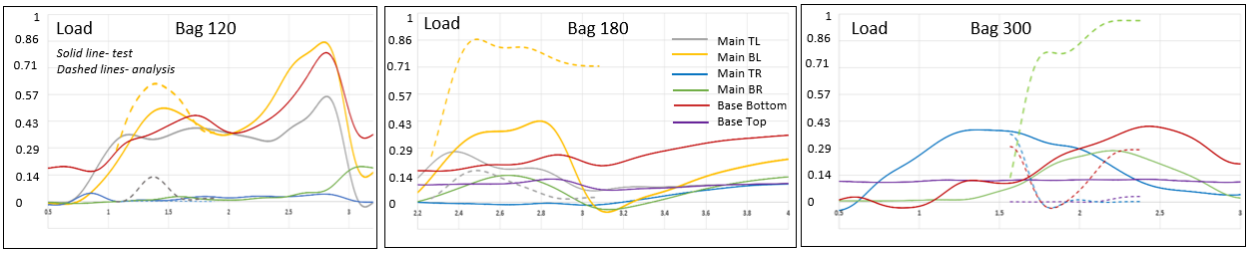


Fig. 10. Comparison of tether loads from calculated (dashed lines) and test (solid lines) data from a flat-water test, with tethers on bag 120, bag 180, and bag 300 plotted from left to right, respectively

The calculated loads were also compared to at-sea loads data collected from full-scale uprighting tests conducted in the Atlantic Ocean in March 2019. Multiple tests were conducted, and the one that was selected for comparison was an uprighting test where the CM was deployed with four of its five bags (the 120º bag was out). The bag out scenario was tested intentionally as part of a check on uprighting performance with a single bag failure. Fig. 11 shows the CM during uprighting and the buoy that recorded the wave height time history. Additional details regarding the test and correlation of the waves to the CM motion is provided in [10].

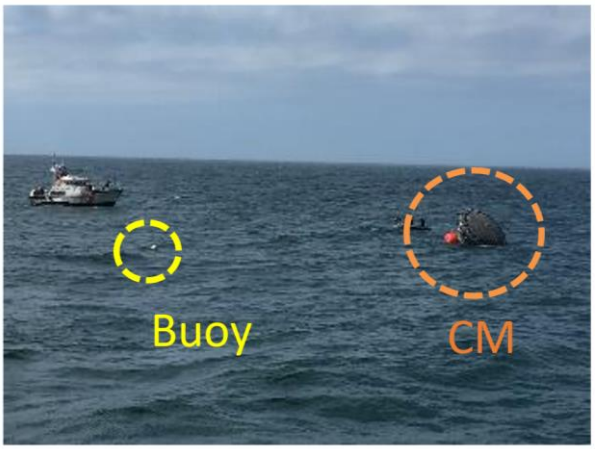


Fig. 11. The measurement buoy and the CM during at-sea test

The wave elevation history recorded by the buoy was prescribed at the boundary of the ALE domain, as described in Section V. Wave elevations calculated in the analysis were largely in phase with the values measured by the buoy, and the calculated elevations were within 20% of the measured wave elevations. Simplifying assumptions in the LS-DYNA model likely contributed to the discrepancy between the ocean wave elevation and the simulated wave elevation. In LS-DYNA, the wave elevation was prescribed at one end of the domain (as shown in Fig. 12) and assumed to propagate from left to right, and the waves could reflect from the walls. The reflection was due to a relatively small domain, necessary to keep the already high computational cost of the model tractable. In the Atlantic data, the source of the wave source came from multiple directions, and the wave propagation was multi-directional as well.

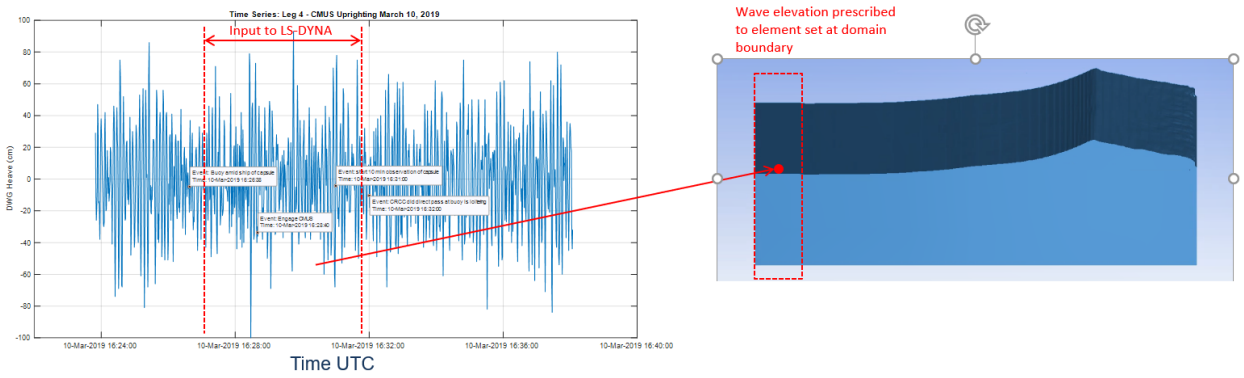


Fig. 12. Time history of the wave height from the buoy deployed in the Atlantic during the uprighting tests (left) and implementation into LS-DYNA (right)

Although there is good agreement between calculation and measurement in the distribution of the loads, the LS-DYNA calculations tended to overpredict main tether loads and underpredict base tether loads. These results are evident in Fig. 13. There were several factors that contributed to this inconsistency. The first was that the bags were fully inflated at the beginning of the calculation, whereas in the test they were inflated slowly during uprighting. Another contributor was the relatively coarse meshes on tethers and gussets which could lead to inaccurate contact between the tethers and the gussets.

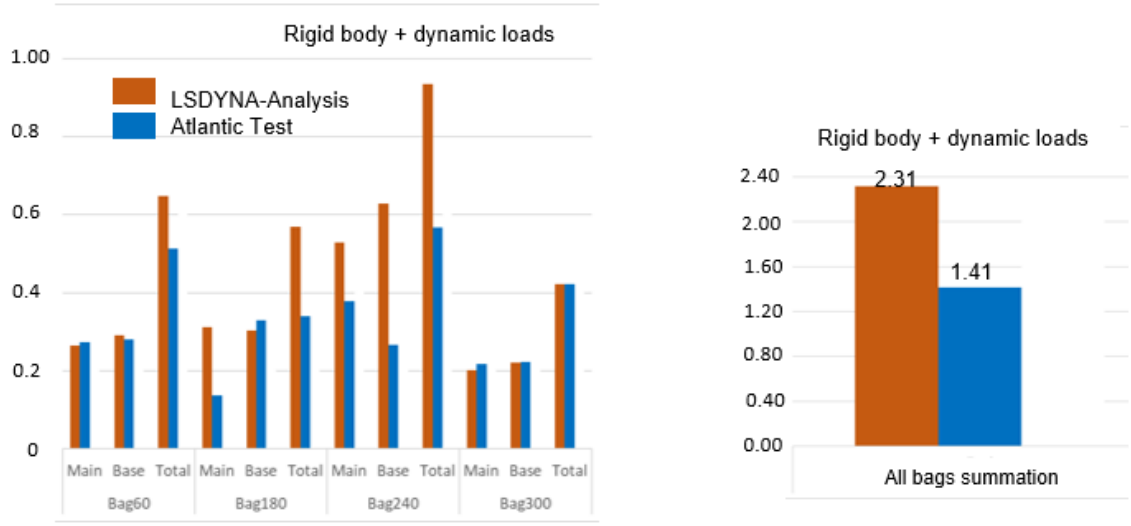


Fig. 13. Comparison of finite element simulation results (orange) and Atlantic test data (blue)

VIII. CMUS Loads Prediction in Ocean Wave Environments

Comparison of the LS-DYNA simulated results with the loads data captured during full-scale uprighting tests discussed in the previous section provided confidence that the LS-DYNA calculations were reasonably accurate and useful for predicting loads. Therefore, uprighting calculations were performed for multiple wave environments defined by DSNE spectra.

Sensitivity analysis was conducted regarding the orientation of the CM relative to the incoming wave direction. It was found that the tether loads are highly dependent on orientation of the CM (yaw axis) with respect to the direction of wave travel. Two orientations examined are shown in Fig. 14. During the study, when the bags pointed toward the waves (figure outlined in orange), the tether loads were less than when the bags pointed away (figure outlined in green). Consequently, the predictive calculations were performed with the bags pointing away so that the predictions would reflect the higher of the two loading scenarios that were evaluated.

Results for two examples, DSNE 4 and DSNE 11, are shown in Fig. 15 and Fig. 16, respectively. For both figures, the loads have been normalized by the peak load for all the tethers.

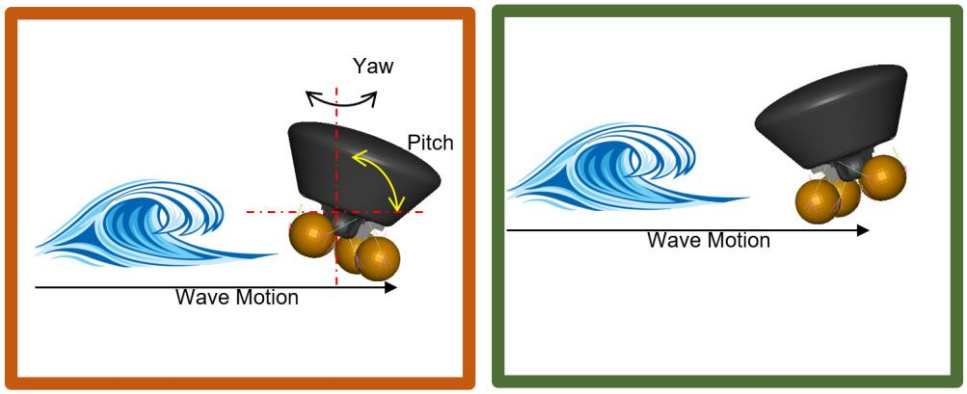


Fig. 14. CM orientation relative wave travel

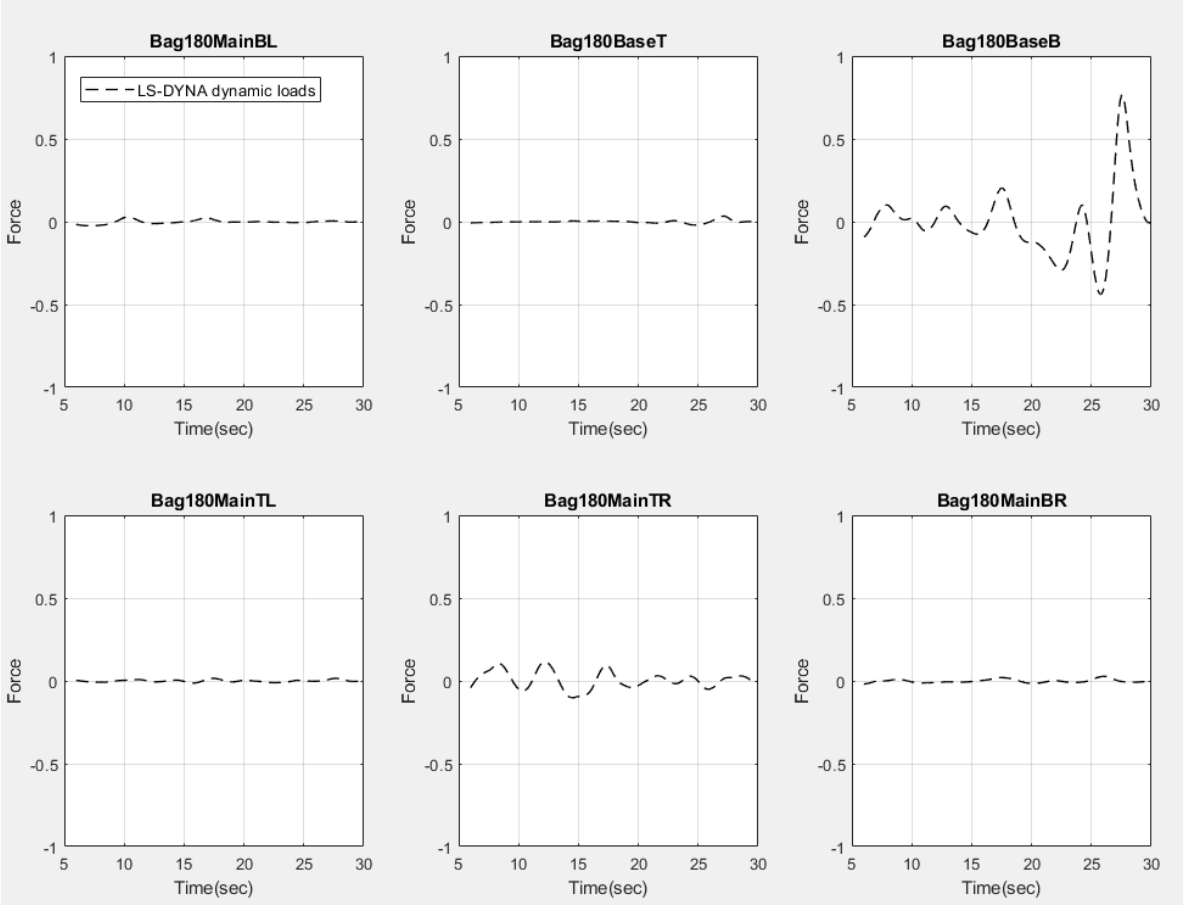


Fig. 15. Predictions of tether load time histories in the DSNE 4 case for bag 180

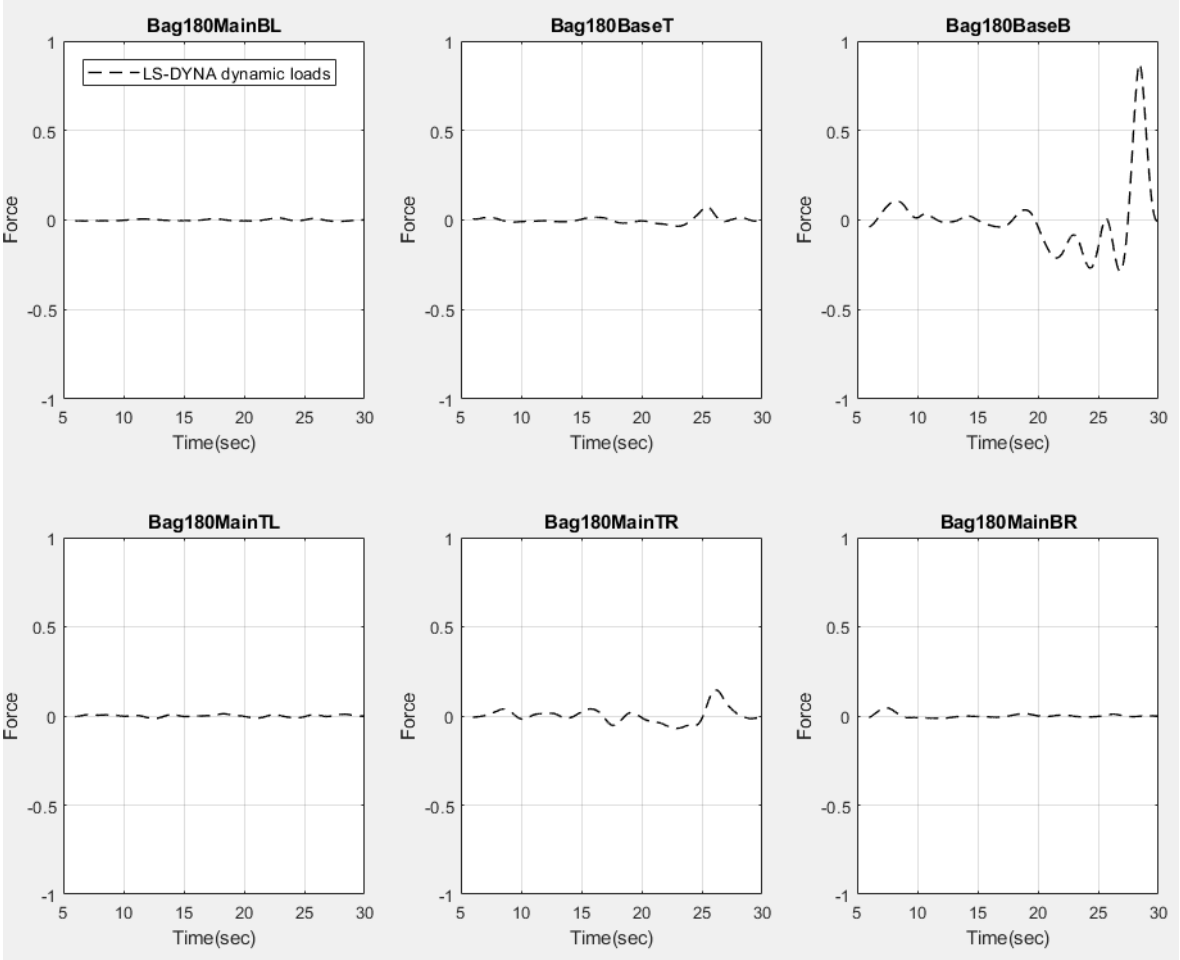


Fig. 16. Predictions of tether load time histories in the DSNE 11 case for bag 180

IX. Conclusion

A continuous multi-body uprighting model was developed for the Orion CM with CMUS in LS-DYNA. Uprighting loads were calculated on the CMUS tethers when subject to design waves that were generated in an ALE domain. A shell and beam model of the CM with the CMUS deployed was included in the domain to calculate CMUS tether loads. Results were compared against existing test data, and the magnitude of tether loads and distribution of loading across tethers calculated in LS-DYNA are consistent with loads measured in uprighting tests of the CM. The LS-DYNA model was used to predict loads on individual CMUS tethers across a broader range of wave conditions.

The ALE method was leveraged to effectively model the fluid dynamics in LS-DYNA, while still relying on a Lagrangian approach to model the structure itself (CM, CMUS bags and CMUS tethers). The inclusion of the ALE method was demonstrated in this paper to be effective for 60-second hydrodynamic calculations despite its more typical usage for shorter transient calculations. Some numerical stability and tether entanglement challenges were observed near the end of the simulation, which could be truncated from the results or mitigated using numerical damping or other means. Competing approaches for modeling hydrodynamics often lack the ability to simultaneously model nonlinear deformation of structures, but ALE was shown to be a feasible method to address the challenge of modeling FSI and deformable structures.

Acknowledgments

The authors would like to acknowledge Karl Kahre from NASA JPL, Jennifer Mann from Johns Hopkins Applied Physics Laboratory, and Bill Milewski from Applied Physical Sciences Corporation for their technical expertise and support during this project. The authors would also like to thank the NASA Engineering and Safety Center for supporting this work under NESC Assessment TI-18-01308.

References

[1] Belytschko, T., Liu, W. K., and Moran, B., *Nonlinear Finite Elements for Continua and Structures*, 2nd ed., Wiley, New York, 2014, Chap. 7

[2] *LS-DYNA Keyword User's Manual, Vol. 1*, Ansys Inc., Canonsburg PA, 2023., URL: https://lsdyna.ansys.com/manuals/

[3] *LS-DYNA Theory Manual*, Ansys Inc., Canonsburg PA, 2023., URL: https://lsdyna.ansys.com/manuals/

[4] Antonia Jaramillo Botero., "Artemis I Update: Orion Secured Inside USS Portland Ahead of Return to Shore," URL: https://blogs.nasa.gov/artemis/author/ajarami1/

[5] Canuto, C., Hussaini, M. Y., Quarteroni, A., Zang, T., *Spectral Methods: Evolution of Complex Geometries and Applications to Fluid Dynamics*, Springer Science and Business Media, 2007.

[6] *LS-DYNA Keyword User's Manual, Vol. 2*, Ansys Inc., Canonsburg PA, 2023., URL: https://lsdyna.ansys.com/manuals/

[7] Kestin, J., Sokolov M., and Wakeham, W., "Viscosity of liquid water in the range −8 °C to 150 °C," *Journal of Physical and Chemical Reference Data*, Vol. 7, No. 3, 1978, pp. 941-948. https://doi.org/10.1063/1.555581

[8] Ducrozet, G., Bonnefoy, F., Le Touzé, D., Ferrant, P. "A modified High-Order Spectral method for wavemaker modeling in a Numerial Wave Tank," *European Journal of Mechanics – B/Fluids*, August 2012

[9] T. VanZwieten, B. Milewski, "Multi-Purpose Crew Vehicle (MPCV) Crew Module (CM) Side Hatch Dynamic Analysis," NESC Final Report, NESC Assessment TI-19-01491, 2023.

[10] I. Bertaska, T. VanZwieten, J. Mann, B. Connell, T. Radke, M. Bernatovich, "Dynamic Characterization of the Crew Module Uprighting System for NASA's Orion Crew Module," IEEE OCEANS Conference, Seattle, WA, 2019.

[11] A. Lockard, T. VanZwieten, J. Mann, M. Keenan, C. Behrend, B. Connell, "NASA's Orion Crew Module Seakeeping Simulation and Test Comparisons in Ocean Wave Environments," IEEE OCEANS Conference, San Diego, CA, 2021.